

基于柔性四羧酸配体构筑的两个镉(II)配位聚合物的晶体结构及荧光性质

刘 露^{*1} 许春莺² 李 英¹ 王吉超¹ 张裕平^{*1} 王键吉³

(¹ 河南科技学院化学化工学院博士后研发基地, 新乡 453003)

(² 洛阳师范学院化学化工学院, 洛阳 471934)

(³ 河南师范大学化学化工学院, 新乡 453003)

摘要: 通过溶剂热和水热合成的方法制备了 2 个 Cd(II) 配位聚合物 $[\text{Cd}_2(\text{L})(\text{DMF})_{1.5}(\text{H}_2\text{O})_2]_n$ (**1**) 和 $[\text{Cd}(\text{L})_{0.5}(4,4'\text{-bpy})(\text{H}_2\text{O})] \cdot 2\text{H}_2\text{O}$ (**2**) ($\text{H}_4\text{L}=5,5'\text{-(己烷-1,6)-双-(氧基)-二-间苯二甲酸}$)。结构分析表明配合物 **1** 是一个(4,4)-连接的 *sql* 拓扑网络, 拓扑符号为 $\{4^4 \cdot 6^2\}_2$ 。配合物 **2** 是一个(4,4,4)-连接的三重穿插的 *bbf* 网络, 拓扑符号为 $(6^6)(6^4 \cdot 8^2)$ 。配合物 **1** 和 **2** 都呈现出较好的热稳定性和荧光性质。

关键词: Cd(II); 晶体结构; 拓扑; 荧光

中图分类号: O614.24²

文献标识码: A

文章编号: 1001-4861(2017)10-1817-08

DOI: 10.11862/CJIC.2017.233

Two Cd(II) Coordination Polymers Based on Flexible Tetracarboxylic Acid Ligands: Crystal Structures and Fluorescent Properties

LIU Lu^{*1} XU Chun-Ying² LI Ying¹ WANG Ji-Chao¹ ZHANG Yu-Ping^{*1} WANG Jian-Ji³

(¹ Postdoctoral Research Base, School of Chemistry and Chemical Engineering, Henan Institute of Science and Technology, Xinxiang, Henan 453003, China)

(² College of Chemistry and Chemical Engineering, Luoyang Normal University, Luoyang, Henan 471934, China)

(³ Henan Normal University, Xinxiang, Henan 453007, China)

Abstract: Two coordination polymers, $[\text{Cd}_2(\text{L})(\text{DMF})_{1.5}(\text{H}_2\text{O})_2]_n$ (**1**) and $[\text{Cd}(\text{L})_{0.5}(4,4'\text{-bpy})(\text{H}_2\text{O})] \cdot 2\text{H}_2\text{O}$ (**2**), have been designed and synthesized by solvothermal or hydrothermal reactions of 5,5'-(hexane-1,6-diyl)-bis(oxy) diisophthalic acid ligand (H_4L) with Cd(II) metal ions in the presence/absence of N-donor ligands. The structures of **1~2** have been determined by single-crystal X-ray diffraction analyses and further characterized via infrared spectra (IR), powder X-ray diffraction (PXRD), elemental analyses and thermogravimetric (TG) analyses. Complex **1** features a (4,4)-connected *sql* topology net with point symbol of $\{4^4 \cdot 6^2\}_2$. Complex **2** presents a trinodal (4,4,4)-connected 3D 3-fold interpenetrating *bbf* network with a Schläfli symbol of $(6^6)(6^4 \cdot 8^2)$. Additionally, complexes **1** and **2** present better thermal stabilities, and show different photoluminescence behaviors in the solid state. CCDC: 1497548, **1**; 1497549, **2**.

Keywords: Cd(II); crystal structure; topology; fluorescence

收稿日期: 2016-12-19。收修改稿日期: 2017-09-07。

河南科技学院高层次人才科研启动项目、河南省博士后科研项目、河南省高等学校重点科研项目(No.16A150007)和河南科技学院标志性创新工程项目(No.2015BZ02)资助。

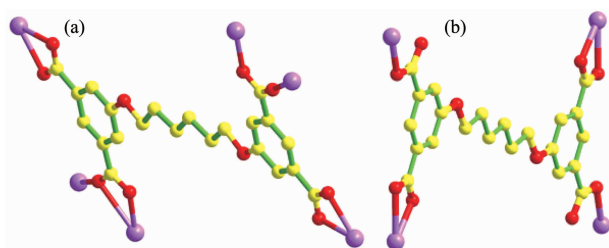
*通信联系人。E-mail: liululiulu2012@126.com, beijing2008zyp@163.com

Metal-organic frameworks (MOFs) have been quickly developed into an active research field and induced considerable attention from both academia and industry, because of their fascinating architectures and distinctive physical properties^[1-12]. The studies in this field have been focused on modifying the building blocks and regulating the assembled motifs for requisite products by choosing disparate organic ligands^[13-14]. Hence, the rationalization design of organic ligands are usually vital for the formation of fresh skeletons. As far as we know, many multidentate aromatic carboxylic acid ligands^[15-17] have been extensively engaged to fabricate coordination complexes on account of their robustness^[18]. Based on the above mentioned, we designed a flexible ligand 5,5'-(hexane-1,6-diyl)-bis(oxy)diisophthalic acid (H_4L) (Scheme 1) as a functional ligand. The H_4L ligand can be deprotonated to the corresponding carboxylate species, which will admit it's all kinds of coordination modes to the inorganic connectors^[19]. In H_4L , the existence of the $(-CH_2-)_n$ spacers and two methoxy groups between the two oxyisophthalic acid fragments will render the carboxyl groups bind with metal ions in different directions, which can offer more possibilities for the construction of versatile frameworks with untouchable functional properties^[20-22].

Given this, the reactions of Cd(II) salts and H_4L were performed in the presence/absence of auxiliary ligand 4,4'-bipyridine (4,4'-bipy). Two different



Scheme 1 Flexible tetracarboxylic acid ligand H_4L



Scheme 2 Schematic view of the versatile coordination modes of the L^{4-} ligand

structural complexes, $[Cd_2(L)(DMF)_{1.5}(H_2O)_2]_n$ (**1**) and $\{[Cd(L)_{0.5}(4,4'-bpy)(H_2O)] \cdot 2H_2O\}_n$ (**2**) have successfully been obtained. Their crystal structures and topological analyses will be represented and discussed. The thermal stabilities and fluorescent properties of **1~2** have also been investigated in detail.

1 Experimental

1.1 Materials and methods

All of the reagents and solvents were commercially practicable. H_4L was synthesized in accordance with a revised procedure from reported literature^[23]. The Fourier transform infrared (FT-IR) spectra were registered on a Bruker-ALPHA spectrophotometer employing KBr pellets within 400~4 000 cm^{-1} scale. Thermogravimetric analyses were implemented adopting a Netzsch STA 449C thermal analyzer with a 10 $^{\circ}C \cdot min^{-1}$ heating speed in the air stream. Elemental analyses of C, H, and N were performed introducing a FLASH EA 1112 analyzer. Powder X-ray diffraction patterns were accomplished on a PANalytical X'Pert PRO diffractometer making use of Cu $K\alpha_1$ radiation ($\lambda=0.154\ 06\ nm$) at 40 kV and 40 mA. The XRD patterns were collected in the range of $5^{\circ}\sim 50^{\circ}$. Diffuse reflectivity spectra of the solid samples were gathered by virtue of a Cary 500 spectrophotometer, which is equipped with a 110 nm diameter integrating sphere. The whole testing is from 200 to 800 nm utilizing barium sulfate ($BaSO_4$) as a standard with 100% reflectance. The luminescence spectra for the powdered solid samples were measured at room temperature on a Hitachi 850 fluorescence spectrophotometer. The excitation slit and emission slit were both 2.0 nm.

1.2 Synthesis of $[Cd_2(L)(DMF)_{1.5}(H_2O)_2]_n$ (**1**)

A mixture of $Cd(NO_3)_2 \cdot 4H_2O$ (0.030 8 g, 0.1 mmol) and L (0.022 3 g, 0.05 mmol) in DMF/ H_2O ($V_{DMF}/V_{H_2O}=2$) was placed in a Teflon-lined stainless steel container (25 mL), and then the vessel was sealed and heated at 85 $^{\circ}C$ for 48 h. After the mixture was cooled to ambient temperature at a rate of 5 $^{\circ}C \cdot h^{-1}$, colorless block-shaped crystals of **1** were obtained with a yield of 62% (based on Cd). Anal. Calcd. for $C_{28}H_{34}Cd_2N_2O_{14}$ (%): C, 39.69; H, 4.04; N, 3.31. Found

(%): C, 39.72; H, 4.03; N, 3.34. IR (KBr, cm^{-1}): 3 415 (m), 3 073(w), 2 943(m), 2 866(w), 1 658(s), 1 542(s), 1 454(m), 1 384(s), 1 318(m), 1 260(m), 1 132(w), 1 042(s), 933(w), 887(w), 812(w), 778(s), 733(s), 673(w).

1.3 Synthesis of $\{[\text{Cd}(\text{L})_{0.5}(\text{4,4'}\text{-bpy})(\text{H}_2\text{O})] \cdot 2\text{H}_2\text{O}\}_n$ (2)

A mixture of $\text{Cd}(\text{NO}_3)_2 \cdot 4\text{H}_2\text{O}$ (0.030 8 g, 0.1 mmol), L (0.022 3 g, 0.05 mmol), 4,4'-bipy (0.007 8 g, 0.05 mmol), and NaOH (0.2 mmol) in H_2O (8 mL) was kept in a 25 mL Teflon-lined stainless steel vessel at 130 $^\circ\text{C}$ for 72 h. After the mixture was cooled to room temperature at a rate of 5 $^\circ\text{C} \cdot \text{h}^{-1}$, colorless rodshaped crystals suitable for X-ray diffraction were obtained with a yield of 75% (based on Cd). Anal. Calcd. for $\text{C}_{21}\text{H}_{23}\text{CdN}_2\text{O}_8$ (%): C, 46.38; H, 4.26; N, 5.15. Found(%): C, 46.34; H, 4.28; N, 5.17. IR (KBr, cm^{-1}): 3 349(m), 3 130(w), 2 871(m), 1 669(m), 1 606(s), 1 549(s), 1 416(s), 1 386(s), 1 324(w), 1 275(m), 1 221(m), 1 125(s), 1 045(s), 886(w), 812(s), 778(s), 733(w), 693(w), 630(s), 518(w).

1.4 Crystal structural determination

The collections of crystallographic data of **1~2** were fulfilled at 293(2) K adopting a Rigaku Saturn

724 CCD diffractometer, which was equipped with Mo $K\alpha$ radiation ($\lambda=0.071\ 073\ \text{nm}$). Absorption corrections were enforced via utilizing multi-scan program. The data were corrected on the basis of Lorentz and polarization effects. The structures were solved by direct methods and refined by full matrix least square on F^2 using the SHELX-97 crystallographic software package^[24]. All of the non-hydrogen atoms were refined anisotropically. All the H atoms were positioned geometrically and refined using a riding model. Crystallographic data and structure refinement details for **1~2** are listed in Table 1.

CCDC: 1497548, **1**; 1497549, **2**.

2 Results and discussion

2.1 Structure description of

$[\text{Cd}_2(\text{L})(\text{DMF})_{1.5}(\text{H}_2\text{O})_2]_n$ (**1**)

X-ray single-crystal diffraction analysis reveals that **1** crystallizes in triclinic space group $P\bar{1}$, generating a 2D layer network. In the structure of complex **1**, the two crystallographically independent Cd(II) ions, one L^{4-} ligand, one and a half associated DMF molecules together with two coordinated water molecules

Table 1 Crystal data and structure refinement details for complexes **1~2**

Complex	1	2
Formula	$\text{C}_{53}\text{H}_{65}\text{Cd}_4\text{N}_3\text{O}_{28}$	$\text{C}_{21}\text{H}_{23}\text{CdN}_2\text{O}_8$
Formula weight	1 641.68	543.81
Crystal system	Triclinic	Monoclinic
Space group	$P\bar{1}$	$P2_1/c$
a / nm	0.760 59(15)	0.871 85(17)
b / nm	1.312 6(3)	1.442 9(3)
c / nm	1.516 1(3)	1.808 0(5)
$\alpha / (^\circ)$	93.93(3)	90.00
$\beta / (^\circ)$	92.16(3)	107.00(3)
$\gamma / (^\circ)$	92.85(3)	90.00
V / nm^3	1.506 9(5)	2.175 1(9)
Z	2	4
$D_c / (\text{g} \cdot \text{cm}^{-3})$	1.809	1.661
μ / mm^{-1}	1.482	1.055
$F(000)$	820.0	1 100
GOF on F^2	1.093	1.067
$R_1 [I > 2\sigma(I)]^a$	0.055 2	0.057 0
wR_2 (all data) ^b	0.119 6	0.104 1

^a $R_1 = \sum \|F_o\| - |F_c| / \sum \|F_o\|$; ^b $wR_2 = [\sum w(F_o^2 - F_c^2)^2 / \sum w(F_o^2)^2]^{1/2}$.

reside in the asymmetric unit. As shown in Fig.1a, the octahedral coordination around Cd1 is provided by four carboxylate oxygens (O3, O13A, O11B and O12B) from three different L^{4-} moieties generating the square base, and the axial coordination is endowed by the DMF oxygen atom (O1) and O2 atom from coordinated water. The 50% ellipsoid figure of **1** is displayed in Fig.1b. The Cd1...O distance ranges from 0.221 8(4) to 0.238 7(4) nm. Cd2 also possesses a distorted octahedral coordination in which the square base is offered by the chelated coordination of the carboxylate oxygen atoms (O5 and O6) from the L^{4-} ligand (Cd2-O5 0.225 7(4), Cd2-O6 0.247 8(4) nm) and the monodentate bridging coordination of the carboxylate oxygen atoms (O4C and O14D) originating from two separate L^{4-} ligands (Cd2-O4C 0.221 8(4); Cd2-O14D 0.227 4(4) nm). Axial coordination comes from one DMF oxygen

atom (O8) (Cd2-O8 0.232 8(5) nm) and one coordinated water oxygen atom (O7) (Cd2-O7 0.230 4(5) nm). Each L^{4-} anion serves as a μ_6 -bridge to connect six Cd(II) ions through its four carboxylate groups, and the coordination mode of $(\kappa^2)-(\kappa^1-\kappa^1)-(\kappa^2)-(\kappa^2-\kappa^1-\mu_2)-\mu_6$ for L^{4-} is found in complex **1** (Scheme 2a). The Cd1 ion and symmetry-related Cd2C (Symmetry codes: C: 2-x, -y, 2-z) ion are bridged by one $\mu_2-\eta^1:\eta^1$ bridging carboxylate group and one $\mu_2-\eta^2:\eta^1$ chelating/bridging carboxylate group to furnish a binuclear $[Cd_2(CO_2)_2]$ unit. Meanwhile, the Cd2 ion and symmetry-related Cd1C ion are also bridged by one $\mu_2-\eta^1:\eta^1$ bridging carboxylate group and one $\mu_2-\eta^2:\eta^1$ chelating/bridging carboxylate group to give a binuclear $[Cd_2(CO_2)_2]$ unit. Within the two bimetallic subunits, the intermetallic distance of Cd...Cd is both 0.393 6 nm. Further expansion of the structure through the L^{4-} anions

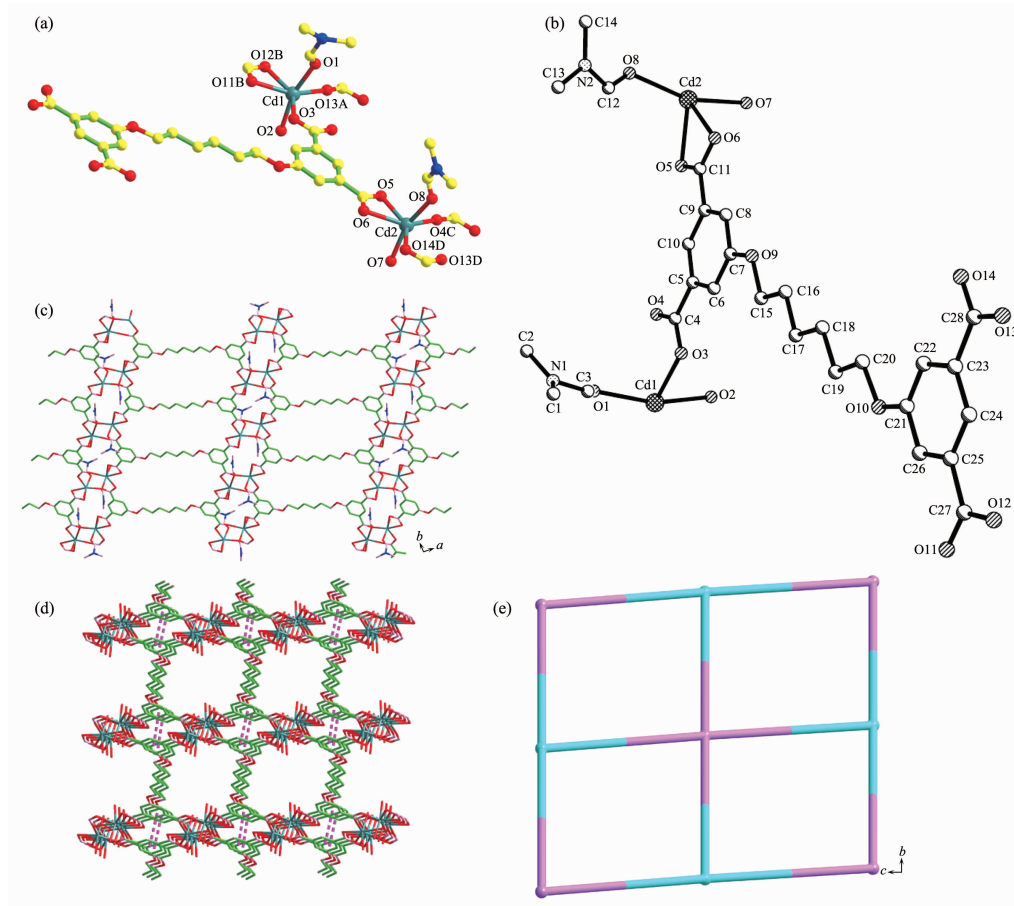


Fig.1 (a) Coordination environment of Cd(II) ion with hydrogen atoms omitted for clarity; (b) 50% ellipsoid figure of **1**; (c) Ladder-like 2D layer structure of **1** viewed along the *c*-axis; (d) 3D supramolecular architecture of **1**; (e) Schematic description of a (4,4)-connected *sql* topology net with point symbol of $\{4^4 \cdot 6^2\}_2$ for **1**

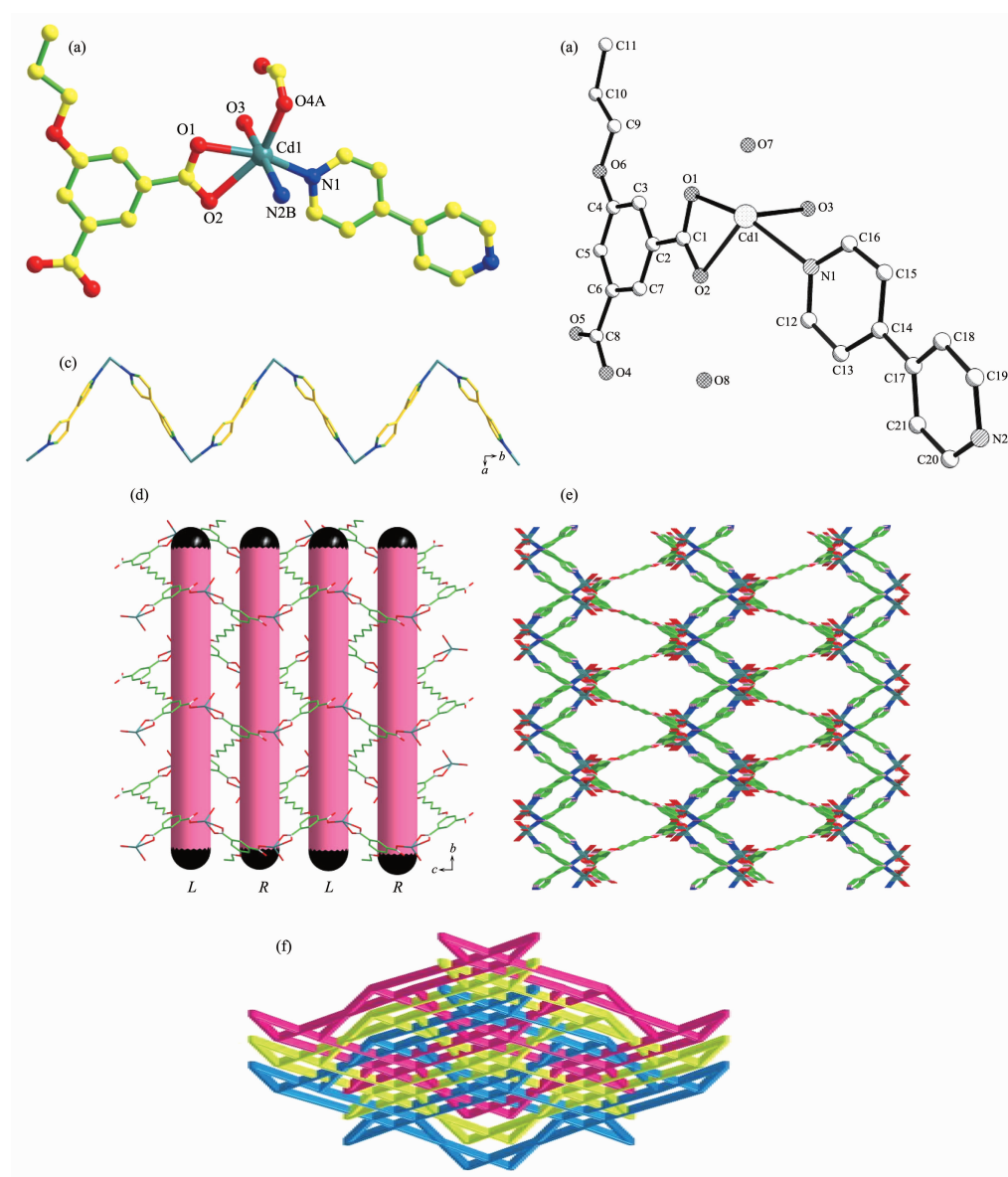
creates a ladder-like 2D layer propagating in *ab* plane (Fig.1c). The cooperative of two kinds of the $\pi \cdots \pi$ stacking interactions (between the two aromatic phenyl rings with a centroid-centroid distance of about 0.366 6 and 0.372 9 nm, respectively) join the adjacent 2D layers into a 3D supramolecular architecture (Fig.1d).

Topologically, the above-mentioned bimetallic subunit can be considered as a 4-connected node since it links four L^{4-} ligands, and the L^{4-} ligand can

be seen as a 4-connector by connecting four bimetallic subunits. Thus, the resulting structure of **1** is described as a (4,4)-connected net with its point (Schläfli) symbol of $\{4^4 \cdot 6^2\}_2$, which is referred to as *sql* topology (Fig.1e).

2.2 Structure description of $\{[Cd(L)_{0.5}(4,4'\text{-bpy})(H_2O)] \cdot 2H_2O\}_n$ (**2**)

Complex **2** is a 3D framework with the monoclinic space group of $P2_1/c$. As depicted in Fig.2a, the asymmetric unit of **2** consists of one Cd(II) ion, half a



Symmetry codes: A: $x, 1.5-y, -0.5+z$; B: $-x, -0.5+y, 0.5-z$

Fig.2 (a) Coordination environment of Cd(II) ion with hydrogen atoms omitted for clarity; (b) 50% ellipsoid figure of **2**; (c) View of the 1D Cd(II)-4,4'-bpy zigzag chain along the *c*-axis; (d) View of the 2D Cd(II)- L^{4-} net built by alternately left-and right-handed helical chains parallel to the *bc* plane; (e) Schematic view of 3D structure of **2**; (f) Schematic representation of the 3-fold interpenetrated topology net for **2**

L ligand, one 4,4'-bpy ligand, one coordinated water molecule and two lattice water molecules. The 50% ellipsoid figure of **2** is displayed in Fig.2b. Each Cd(II) ion is six-coordinated by three carboxylate oxygen atoms (O1, O2 and O4A) from two L^{4-} anions, one oxygen atom (O3) from one coordinated water molecule and two nitrogen atoms (N1 and N2B) from two 4,4'-bpy ligands, in turn, forming a distorted octahedral geometry. The O1, O2, O4A and N1 atoms comprise the equatorial plane, and the O3 and N2B atoms occupy axial positions. The Cd-O bond distances vary from 0.222 1(3) to 0.246 9(3) nm, while the Cd-N1 and Cd-N2B bond lengths are 0.230 8(3) and 0.234 3(4) nm, respectively. The bond angles around Cd1 range from 54.85(1)° to 169.65(1)°.

In **2**, each 4,4'-bpy ligand bridges two Cd(II) ions to product a 1D zigzag chain with a Cd...Cd distance of 1.161 4 nm propagating along the *c*-axis (Fig.2c). The L^{4-} anions connects four Cd(II) cations, where two carboxylate groups take $\mu_1\text{-}\eta^1\text{:}\eta^1$ coordination modes, the other two carboxylate groups adopt $\mu_1\text{-}\eta^1\text{:}\eta^0$ fashions (Scheme 2b). The Cd(II) ions are bridged by the L^{4-} anions to generate a 2D sheet with alternately arranged left- and right-handed helical chains along the *a*-axis (Fig.2d). The screw axes of these helices are all parallel to the *b*-axis, and the pitch is 1.442 9(3) nm. The Cd(II)- L^{4-} 2D layers are pillared by 1D Cd(II)-4,4'-bpy chain through sharing the common Cd(II) ions to result in the formation of a 3D framework (Fig.2e). Three identical nets are further interpenetrating with each other, leading to the formation of the final 3-fold interpenetrating network (Fig.2f). To get deep insight into the structure of **2**, the topological analysis was carried out. The Cd(II) ion can be assigned to a 4-connected node, linking with two L^{4-} anions and two 4,4'-bpy ligands. The L^{4-} ligands connect four Cd(II) ions. Thus, the L^{4-} ligands are considered as 4-connected linkers. Finally, the 3D framework presents a binodal (4,4)-connected *bbf* topology with the Schläfli symbol of $(6^6)(6^4\cdot 8^2)$ (Fig.2f).

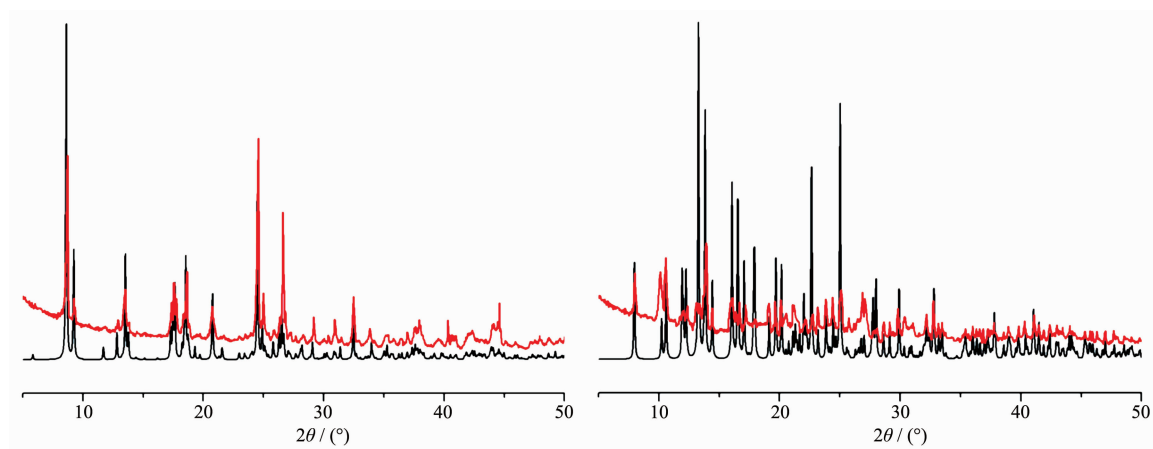
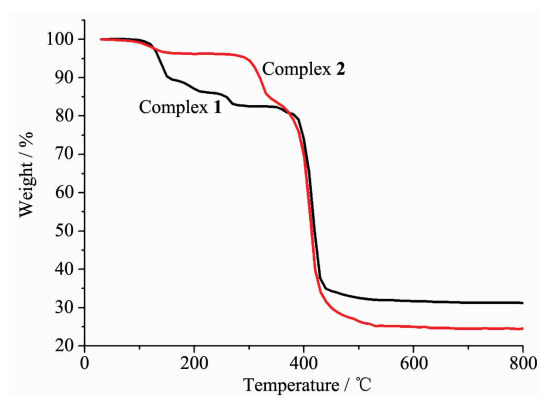
2.3 Effects of the coordination modes of the L^{4-} anion and 4,4'-bpy ligand on the frameworks of complexes 1~2

On the basis of the structure descriptions of 1~2,

we find that the L^{4-} anion can adopt miscellaneous coordination modes, linking to six (complex **1**) or four (complex **2**) metal ions. The structural diversities of 1~2 can be attributed to the various coordination modes of carboxylate groups in the H_4L molecule. For **1**, the carboxylate group of L^{4-} anion bond with the metal ions in a $(\kappa^2)\text{-(}\kappa^1\text{-}\kappa^1\text{)}\text{-(}\kappa^2\text{)}\text{-(}\kappa^2\text{-}\kappa^1\text{-}\mu_2\text{)}\text{-}\mu_6$ fashion. This kind of coordination fashion in **1** brings about the formation of a ladder-like 2D layer Cd- L^{4-} net. For **2**, two carboxylate groups of L^{4-} anion take $\mu_1\text{-}\eta^1\text{:}\eta^1$ coordination modes, while the other two carboxylate groups adopt $\mu_1\text{-}\eta^1\text{:}\eta^0$ fashions. This kind of coordination fashion in **2** afford a 2D Cd- L^{4-} net with alternately arranged left- and right-handed helical chains. The N-donor ligands have also a far-reaching influence on the final structures of the complexes. In **2**, The 4,4'-bpy bridge Cd(II) ions to generate a 1D infinite chain. The Cd- L^{4-} 2D layers are connected by Cd(II)-4,4'-bpy 1D chain inducing a 3-fold interpenetrating 3D architecture.

2.4 XRD patterns and thermal analyses

The PXRD patterns of complexes 1~2 are shown in Fig.3. The PXRD patterns of the two complexes determined by experiment are in line with the simulated ones of single crystals, which indicates that each of the two complexes is pure phase. To appraise the stability of the coordination architectures, thermogravimetric analyses (TGA) of 1~2 were carried out (Fig.4). The TGA curve of complex **1** exhibits that it loses weight from 114 to 273 °C, corresponding to the decomposition of two coordinated water molecules and one and a half associated DMF molecules (Obsd. 17.35%; Calcd. 17.74%). The decomposition of L^{4-} is observed in the range of 375~527 °C. A residue of CdO (Obsd. 31.26%, Calcd. 31.29%) is discovered. The TGA data of complex **2** display a two-step weight loss. The first weight loss of 3.75% is observed in the temperature range of 84~156 °C, which corresponds to the loss of two lattice water molecules and one coordinated water molecule (Calcd. 3.31%). The second step weight loss from 259~497 °C corresponds to the decomposition of L^{4-} and 4,4'-bpy, accompanying with the CdO residue of 24.52% (Calcd. 23.61%).

Fig.3 Experimental (top) and simulated (bottom) PXRD patterns of complexes **1~2**Fig.4 TGA curves of complexes **1~2**

2.5 Diffuse-reflectance UV-Vis spectra and photoluminescence properties

As depicted in Fig.5 and Table 2, diffuse-reflectance UV-Vis spectrum of the ligand H_4L demonstrates two intense absorption bands ($\lambda_{\max}=257, 328$ nm) in the range of 200~400 nm, which are assigned to the typical $\pi \rightarrow \pi^*$ transitions^[25-27]. Besides, the

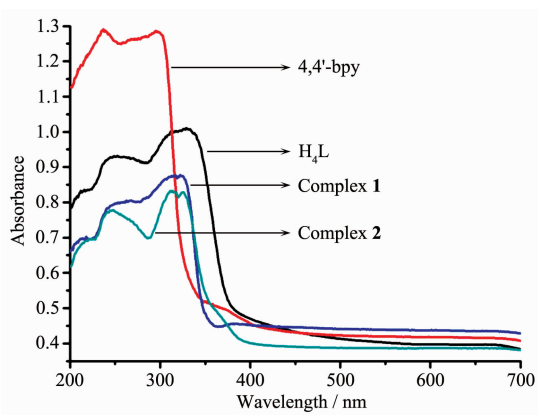
Fig.5 UV-Vis absorption spectra at room temperature for the free organic ligands and complexes **1~2**

Table 2 Main absorption bands for the free organic ligands and complexes **1~2**

Sample	λ_{\max} / nm
H_4L	257, 328
4,4'-bpy	236, 297
Complex 1	212, 248, 313, 321
Complex 2	214, 245, 311, 325

UV-Vis absorption spectra of 4,4'-bpy manifest 236 and 297 nm absorption bands in the scale of 200~400 nm. In accordance with the relevant literatures^[28], the absorption bands of 4,4'-bpy belong to the $\pi \rightarrow \pi^*$ transitions of the aromatic rings. Complexes **1~2** display the analogous absorption bands, which are also extremely similar to the peak of H_4L . Besides, the lowest energy absorption band of 4,4'-bpy are larger than that of H_4L in the energy level, which indicates that 4,4'-bpy might have less influence than the lowest energy absorption band of H_4L through the coordination with the metal ion. For **1** and **2**, their lowest energy absorption bands show smaller hypochromatic shift (7 and 3 nm, respectively), comparing with that of H_4L . The situation may be attributed to the coordination of the H_4L to the Cd(II) ion increasing the energy gap of the intraligand (IL, $\pi \rightarrow \pi^*$) transition.

Moreover, the solid-state luminescences of complexes **1~2** and the free ligand H_4L are also surveyed at ambient temperature. As reported before^[29-30], the emission of 4,4'-bpy is 428 nm ($\lambda_{\text{ex}}=350$ nm). The photoluminescent spectrum of H_4L exhibits a weak emission at 429 nm ($\lambda_{\text{ex}}=330$ nm, Fig.6), which is very close to

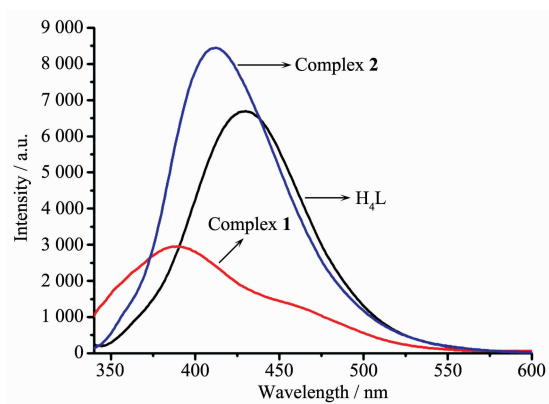


Fig.6 Solid-state photoluminescent spectra of complexes **1~2** and free ligands

that of 4,4'-bipy. For complex **1**, excited at 321 nm, it gives rise to an emission band at 389 nm (Fig.6). As compared to the H₄L ligand, a hypochromic shift (40 nm) is observed. The emission spectrum of complex **2** (λ_{em} =412 nm, λ_{ex} =319 nm) is blue-shifted (17 and 16 nm) corresponding to those of H₄L and 4,4'-bipy, respectively. Illustrated by the Fig.6, the emission spectra of **1~2** are parallel to that of the H₄L ligand, which also be mainly attributed to the intraligand emission of H₄L^[31].

3 Conclusions

In brief, two Cd(II)-L⁴⁻ coordination complexes with captivating frameworks and topologies have been successfully constructed under hydrothermal/solvothermal conditions. The structural diversities of complexes **1~2** indicate that the conformation of the H₄L ligand containing six carbon aliphatic backbone and 4,4'-bipy coligand play key roles in the assembly of the final structure.

References:

- [1] Zheng A X, Si J, Tang X Y, et al. *Inorg. Chem.*, **2012**,**51**: 10262-10273
- [2] Jiang H, Feng D, Liu T, et al. *J. Am. Chem. Soc.*, **2012**,**134**: 14690-14693
- [3] Suh M. P, Park H. J, Prasad T. K, et al. *Chem. Rev.*, **2012**, **112**:782-835
- [4] Li J, Sculley R J, Zhou H C. *Chem. Rev.*, **2012**,**112**:869-932
- [5] Liu Y, Xuan W, Cui Y. *Adv. Mater.*, **2010**,**22**:4112-4135
- [6] Nugent P S, Rhodus V L, Pham T, et al. *J. Am. Chem. Soc.*, **2013**,**135**:10950-10953
- [7] Bauer C A, Timofeeva T V, Settersten T B, et al. *J. Am. Chem. Soc.*, **2007**,**129**:7136-7144
- [8] Zhang C L, Zhang M D, Qin L, et al. *Cryst. Growth Des.*, **2014**,**14**:491-499
- [9] Cui Y, Yue Y, Qian G, et al. *Chem. Rev.*, **2012**,**112**:1126-1162
- [10] Cook T R, Zheng Y R, Stang P J. *Chem. Rev.*, **2013**,**113**: 734-777
- [11] Peng Y, Gong T, Cui Y. *Chem. Commun.*, **2013**,**49**:8253-8255
- [12] Wang Y L, Fu J H, Wei J J, et al. *Cryst. Growth Des.*, **2012**, **12**:4663-4668
- [13] Kanoo P, Gurunatha K L, Maji T K. *Cryst. Growth Des.*, **2009**,**9**:4147-4156
- [14] Hargman P J, Hargman D, Zubietta J. *Angew. Chem., Int. Ed.*, **1999**,**38**:2638-2684
- [15] Zhang X P, Zhou J M, Shi W, et al. *CrystEngComm*, **2013**, **15**:9738-9744
- [16] Liu W L, Yu J H, Jiang J X, et al. *CrystEngComm*, **2011**, **13**:2764-2773
- [17] Ordonez C, Fonari M, Lindline J, et al. *Cryst. Growth Des.*, **2014**,**14**:5452-5465
- [18] Eddaoudi M, Moler D B, Li H, et al. *Acc. Chem. Res.*, **2001**,**34**:319-330
- [19] Karmakar A, Goldberg I. *CrystEngComm*, **2011**,**13**:339-349
- [20] Hawxwell S M, Espallargas G M, Bradshaw D, et al. *Chem. Commun.*, **2007**:1532-1534
- [21] Perry J J, Kravtsov V C, McManus G J, et al. *J. Am. Chem. Soc.*, **2007**,**129**:10076-10077
- [22] Qu L L, Zhu Y L, Li Y Z, et al. *Cryst. Growth Des.*, **2011**, **11**:2444-2452
- [23] Berl V, Schmutz M, Krische M J, et al. *Chem. Eur. J.*, **2002**, **8**:1227-1244
- [24] Sheldrick G M. *Acta Crystallogr., Sect. A: Found. Crystallogr.*, **2008**,**A64**:112-122
- [25] He Y H, Feng Y L, Lan Y Z, et al. *Cryst. Growth Des.*, **2008**,**8**:3586-3594
- [26] Zhang L Y, Zhang J P, Lin Y Y, et al. *Cryst. Growth Des.*, **2006**,**6**:1684-1689
- [27] Zhang R B, Li Z J, Qin Y Y, et al. *Inorg. Chem.*, **2008**,**47**: 4861-4876
- [28] Ohkoshi S, Tokoro H, Hozumi T, et al. *J. Am. Chem. Soc.*, **2006**,**128**:270-277
- [29] Censo D D, Fantacci S, Angelis F D, et al. *Inorg. Chem.*, **2008**,**47**:980-989
- [30] Stadler M, Puntoriero F, Campagna S, et al. *Chem. Eur. J.*, **2005**,**11**:3997-4009
- [31] Fang S M, Chen M, Yang X G, et al. *CrystEngComm*, **2012**, **14**:5299-5304